

NRL Report 5930

UNCLASSIFIED

IN-PILE HALL COEFFICIENT AND CONDUCTIVITY MEASUREMENTS ON ZONE-REFINED P-TYPE SILICON

G. C. Bailey and C. M. Williams

Metal Physics Branch
Metallurgy Division

May 13, 1963



U. S. NAVAL RESEARCH LABORATORY
Washington, D.C.

CONTENTS

Abstract ii
 Problem Status ii
 Authorization ii

INTRODUCTION 1

EXPERIMENTAL TECHNIQUES 1

RESULTS AND DISCUSSION 2

 Approach to Intrinsic Conductivity 2
 Detailed Variation of Conductivity with Integrated Fast Flux . 5
 Hall Coefficient Variation with Integrated Fast Flux;
 Hole Removal Rates 7
 Hall Mobility 9

SUMMARY 10

ACKNOWLEDGMENTS 11

REFERENCES 11

ABSTRACT

The Hall coefficient and conductivity have been measured during pile irradiation for a number of zone-refined p-type silicon crystals with initial resistivities of 1, 8, and 100 ohm-cm. To supply the magnetic field (500 oersteds) for the Hall measurements in the reactor, a small electromagnet was used. The conductivity of zone-refined silicon shows much faster changes with irradiation than pulled silicon samples of equivalent resistivity. The 100-ohm-cm samples exhibit a monotonic nonlinear decrease of $\ln \sigma$ (conductivity) vs ϕ_f (integrated fast flux), whereas the other samples with initial Fermi levels closer to the valence band have one or two regions of linear decrease in $\ln \sigma$ vs ϕ_f before the nonlinear decrease region is observed. The Hall mobility for the 100-ohm-cm samples decreases and becomes negative as a result of the carrier density decreasing with irradiation. In the case of the 8-ohm-cm sample, the Hall mobility decreases with irradiation, whereas the 1-ohm-cm sample shows no change in Hall mobility with irradiation up to the maximum integrated flux used in the present experiment. The origins of the dependence of $\ln \sigma$ on ϕ_f as well as the behavior of the Hall coefficient and Hall mobility with irradiation are discussed.

PROBLEM STATUS

This is an interim report on the problem;
work is continuing.

AUTHORIZATION

NRL Problem M01-10
Project RR 007-01-46-5408

Manuscript submitted February 19, 1963.

IN-PILE HALL COEFFICIENT AND CONDUCTIVITY MEASUREMENTS ON ZONE-REFINED P-TYPE SILICON

REPRODUCED FROM
NBS MONOGRAPH
NO. 10

INTRODUCTION

Radiation damage studies of single-crystal silicon have been in progress for a number of years and have revealed many interesting features. These include the existence and location of discrete energy levels (1-10) formed in the forbidden band by various kinds of incident irradiation (electrons, deuterons, neutrons, and gamma rays). An analysis of the radiation damage is usually accomplished by observing the postirradiation temperature dependence of the Hall coefficient, the electrical conductivity, and the optical absorption. But perhaps the most powerful tool used to study defect centers is electron spin resonance taken in conjunction with optical absorption. Using this technique, it has been shown quite conclusively (11,12) that the Si-A center, which is responsible for the electron trapping level (0.17 eV below the conduction band in electron-irradiated pulled silicon), is a combination of a vacancy and an oxygen atom.

In contrast to most of the previous work which has been carried out on pulled silicon, having about 10^{18} oxygen atoms per cm^3 , the present experiments were set up to measure the effect of neutron irradiation on the Hall coefficient and conductivity of zone-refined silicon, which has less than 10^{16} oxygen atoms per cm^3 (13). Furthermore, the experiments were designed to be carried out during pile irradiation in the reactor, whereas all previous Hall coefficient measurements on neutron-irradiated silicon (5,6,9,14,15) have been made after irradiation.* Buras and Suwalski (16), however, have made in-pile Hall coefficient measurements on germanium.

In this report, after the experimental techniques of measurement have been discussed, the experimental findings will be divided into four main headings: the approach of the samples to intrinsic conductivity, the variation of conductivity with integrated flux, the Hall coefficient variation and hole removal rates, and, finally, the variation of Hall mobility as a function of integrated flux.

EXPERIMENTAL TECHNIQUES

Samples with dimensions $1 \times 0.2 \times 0.2$ cm were cut from uncompensated zone-refined single crystals of p-type silicon (doped with boron) purchased from Merck and Company. The long axis of each sample was in the (111) direction. The samples were etched in CP-4, sandblasted with an industrial airbrasive unit, and then gold plated. A jig which covered the ends and four points (two for conductivity probes and two for Hall coefficient probes) of the individual crystals was used while excess gold plate was sandblasted away. The crystals were placed in transite holders between the poles of a small electromagnet. The magnetic field was maintained at a rather low but sufficient value of 500 oersteds. Samples B-1, D-8 and G-100[†] were all irradiated at 100°C with the following exception: the temperature of D-8 varied as the ambient reactor temperature and was 79°C initially, 93°C at 90×10^{12} n/cm², and 100°C after 195×10^{12} n/cm². Samples

*This is true with the possible exception of Wertheim's study (5) of fission plate-irradiated silicon.

[†]The number in the sample designation refers to the preirradiation room temperature resistivity in units of ohm-cm.

H-100 and J-100 were irradiated at 72°C in the presence of a dry helium atmosphere. Other details of the irradiation procedure are described in an earlier paper (17).

The measuring equipment consisted of a sensitive potentiometer with an electronic null detector. By means of a suitable switching arrangement the null detector was connected either across the galvanometer output of the potentiometer or in series with the source. Very high sensitivity was obtained with the null detector in series with the source and this was especially needed as irradiation proceeded and the source resistance increased. With a 100-ohm-cm sample, for instance, the source resistance varied during irradiation from 500 ohms to above 50,000 ohms. With this apparatus, five quantities were measured: the Hall potential, the potential across the resistivity probes, the sample current, the temperature, and the current through the magnet coils. From these observations, the Hall coefficient and resistivity were calculated.

The flux for samples B-1 and D-8, irradiated at the centerline of the core, was 3.3×10^{10} n/cm² sec and was measured using activity determinations of monitors of sulfur (2.9-Mev threshold) pellets irradiated with the samples. Samples G-, H-, and J-100 were placed 1 foot, 3.4 feet, and 4 feet above the core centerline. For these samples, the flux was determined by a separate experiment, taking the centerline core flux to be that as found for samples B-1 and D-8. Several sulfur pellets were placed at intervals above the core centerline, and the resultant log activity vs distance plot gave fluxes for G-, H-, and J-100 of 1.1×10^{10} , 1.1×10^9 , and 3.6×10^8 n/cm² sec, respectively.* The reactor power level for samples B-1, D-8, and G-100 was 100 kw whereas for H- and J-100, the power was 1 Mw. This way of determining the flux values for H- and J-100 assumes that the log activity vs distance plots for the reactor operating at 100 kw and 1 Mw have the same slopes.

RESULTS AND DISCUSSION

Approach to Intrinsic Conductivity

The conductivity of all the samples decreases as a function of integrated fast flux and tends toward some limiting value as shown in Fig. 1. This value, σ_L , is tabulated in Table 1 along with the calculated value of σ_i , the intrinsic conductivity at the temperature of measurement. Values of σ_i were obtained from (18)

$$\sigma_i = p_i e(\mu_e + \mu_h) \quad (1)$$

where p_i is the density of holes in the intrinsic region and μ_e and μ_h are the electron and hole conductivity mobilities respectively. If one uses the empirical expressions for the conductivity mobilities and for p_i as obtained by Morin and Maita (19), one obtains

$$\sigma = \left(1.5 \times 10^{33} T^3 e^{-1.21/kT}\right)^{1/2} e \left[1450 \left(\frac{300}{T}\right)^{2.6} + 500 \left(\frac{300}{T}\right)^{2.3}\right]. \quad (2)$$

The temperature range over which Eq. (2) is valid is that for which lattice scattering is the main scattering mechanism. According to Conwell (20) the impurity contribution to the mobilities of the samples used (10^{16} , 10^{15} , 10^{14} impurity atoms/cm³) is small. The influence of radiation-induced defects on the scattering may be estimated as follows. If one takes ten displaced atoms/cm³ per neutron/cm²,[†] the total density of displaced

*The assumption is made that the integrated flux, and not the flux, is the important parameter.
[†]A value of 37 cm⁻¹ was calculated for silicon using the method of Ref. 21. This value was arbitrarily reduced to 10 cm⁻¹ on the basis of a statement also in Ref. 21, p. 36, to the effect that the ratio of calculated to observed numbers of defects "seems to lie in the range of 3 to 10 for most materials."

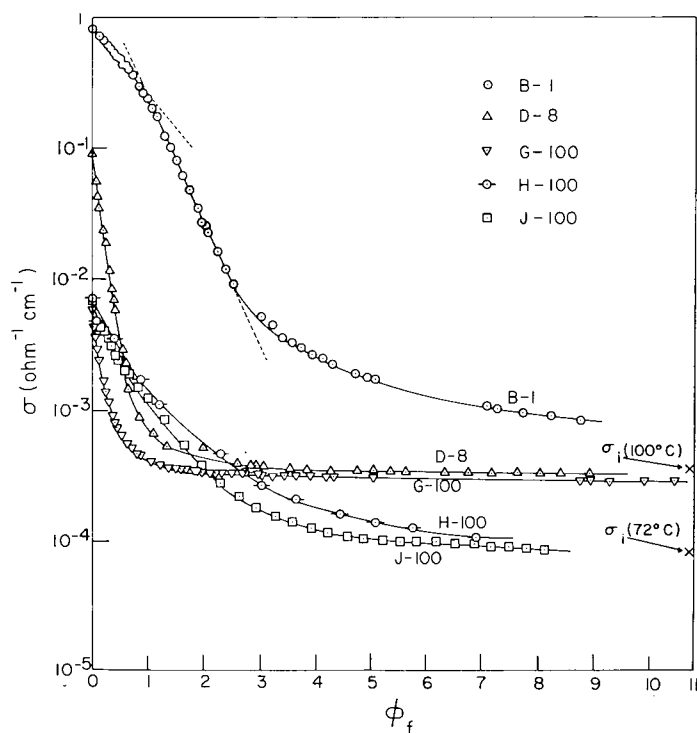


Fig. 1 - Conductivity σ as a function of integrated fast flux ϕ_f for different p-type silicon samples irradiated at 100°C (B-1, D-8, G-100) and at 72°C (J-100, H-100). The crosses are values of σ_i calculated from Eq. (2). To obtain the abscissas of points in n/cm^2 , multiply the numbers along the abscissa axis by 2×10^{14} (B-1, D-8), 5×10^{13} (G-100), 2×10^{12} (J-100), and 10^{12} (H-100). Some of the points are very low integrated flux for sample B-1 have been omitted for the sake of clarity.

atoms N_d at the end of irradiation is found and the values are given in Table 1. The largest value of N_d is $1.8 \times 10^{16}/cm^3$, which is about the same as the initial chemical impurity concentration for B-1. Since an initial impurity concentration of $10^{16}/cm^3$ does not have much effect on the mobility, neither should the radiation-induced defects, and the use of Eq. (2) seems quite reasonable. This is more a plausibility argument than a proof, since one should really measure μ_e and μ_h as a function of irradiation.

It is clear from comparison of σ_L and σ_i in Table 1 that samples D-8 and G-100 have become intrinsic, H-100 and J-100 are almost intrinsic, and sample B-1 is not intrinsic. It is to be noted that when the sample becomes intrinsic the density of displaced atoms is 10 times the initial hole density p_0 , also given in Table 1. The significance, if any, of this factor of 10 is not known at present. The purer the sample, the smaller is the initial carrier density, and the smaller is the integrated fast flux necessary to make the sample go intrinsic. (Compare D-8 with G-100 both irradiated at 100°C.) Also, the lower the temperature, the smaller is the integrated flux needed to make the sample become intrinsic. (Compare G-100 with H- or J-100.)

Table 1
Sample Characteristics and Irradiation Data*

Sample	ρ_0 (ohm-cm)	P_0 (holes/cm ³)	σ_L (ohm ⁻¹ cm ⁻¹)	σ_i (ohm ⁻¹ cm ⁻¹)	$E_f - E_v$ (ev)	N_d (atoms/cm ³)	ϕ_{f1} (n/cm ²)	α (cm ⁻¹)	$P_h(E = 1.6 \text{ ev})$	$P_h(E = 0.30 \text{ ev})$	ϕ (n/cm ² sec)	T (°C)
B-1	1	1.9×10^{16}	8.0×10^{-4}	3.5×10^{-4}	0.21	1.7×10^{16}	--	$\begin{cases} 80 \\ 40 \end{cases}$	0.17	0.94	3.3×10^{10}	100
D-8	8	1.7×10^{15}	3.2×10^{-4}	3.5×10^{-4}	0.27	1.8×10^{16}	1.0×10^{14}	60	0.026	0.72	3.3×10^{10}	79-100
G-100	100	1.4×10^{14}	2.8×10^{-4}	3.5×10^{-4}	0.37	5.2×10^{15}	2.6×10^{13}	20	0.0014	0.10	1.1×10^{10}	100
H-100	100	1.3×10^{14}	1.0×10^{-4}	8.1×10^{-5}	0.34	2.9×10^{14}	4.5×10^{12}	115	0.0023	0.21	1.1×10^9	72
J-100	100	1.2×10^{14}	8.5×10^{-5}	8.1×10^{-5}	0.34	1.6×10^{14}	6.4×10^{12}	140	0.0023	0.21	3.6×10^8	72

* ρ_0 = nominal room temperature resistivity; P_0 = initial density of positive carriers (holes); σ_L = limiting conductivity near end of irradiation; σ_i = intrinsic conductivity calculated from Eq. (2); $E_f - E_v$ = initial Fermi energy E_f minus the energy of the top of the valence band E_v calculated from Eq. (3); N_d = calculated total number of displaced atoms per cm³; ϕ_{f1} = integrated flux at which the sample conductivity is $2\sigma_i$; α = removal rate; $P_h(E)$ = calculated probability of occupancy of levels at $E = 0.16$ ev and 0.30 ev by holes; ϕ = flux; T = irradiation temperature.

To compare the data of this paper with that of other workers, it is convenient to use the value of the integrated flux ϕ_{f_1} at which σ equals $2\sigma_i$; these values are tabulated in Table 1. Crawford and Cleland (22) observed the behavior of the approach to intrinsic conductivity of pile-irradiated n-type and p-type pulled silicon having initial resistivities of 0.8 ohm-cm and 5 ohm-cm respectively. Their p-type silicon irradiated at 60°C was within a factor of 2 of being intrinsic after 1×10^{17} n/cm². This is a factor of 10^3 greater integrated flux than the value for the 8-ohm-cm sample irradiated at a slightly higher temperature in the present experiment. Longo (14) irradiated 2-ohm-cm n-type and 12-ohm-cm p-type pulled silicon in a reactor and found the samples to have resistivities corresponding to intrinsic material following the irradiation at 45°C. His quoted integrated flux after irradiation was 7×10^{17} n/cm². Thus, with respect to the approach to intrinsic conductivity, zone-refined and pulled silicon crystals of equivalent resistivity behave in the same manner except that zone-refined silicon approaches intrinsic conductivity with much less irradiation than pulled silicon. This agrees with a footnote statement of Watkins et al. (23), who made measurements of electron-irradiated silicon.

Detailed Variation of Conductivity with Integrated Fast Flux

Sample B-1 - Figure 1 shows that the initial behavior of B-1 is different from that of D-8 and the 100-ohm-cm samples. For sample B-1, there are initially two linear regions of $\ln \sigma$ vs ϕ_f . (To make certain that a similar behavior was not missed in the two 100-ohm-cm samples because of the rapid change of σ with ϕ_f , a third 100-ohm-cm sample, J-100, was irradiated at a very low flux of 3.6×10^8 n/cm² sec. The conductivity data shown for this sample was taken over a period of 780 minutes, and a monotonic nonlinear decrease of $\ln \sigma$ with ϕ_f was observed.)

To help explain the behavior of the conductivity as a function of integrated fast flux for sample B-1 (and for the other samples as well), we will examine the variation of the Fermi energy with integrated flux. Analysis of the Hall data reveals for sample B-1 that $\ln p$ vs ϕ_f , where p is the hole density, also has two linear regions. Furthermore, the hole density is related to the Fermi energy E_f by use of (24)

$$E_f - E_v = kT \ln \left[2 \left(\frac{2\pi m_h kT}{h^2} \right)^{3/2} \frac{1}{p} \right] \quad (3)$$

where m_h is the density-of-states mass for the holes in the valence band and E_v is the energy of the top of the valence band. Therefore, since $\ln p$ vs ϕ_f is linear, E_f vs ϕ_f will also be linear. In addition, we assume that the lower half of the forbidden band has defect levels similar to those in the neutron-irradiated pulled silicon observed by Klein and Straub (6); that is, there are levels at 0.16 eV and 0.30 eV above the valence band.* The density of holes trapped by the defects at a given temperature depends on the probability of occupancy of the level and the net rate at which the defects are formed. The probability of occupancy, shown in Table 1, is calculated from

$$\left[1 + e^{(E_f - E)/kT} \right]^{-1}$$

and is 0.17 and 0.94 for the 0.16-eV and 0.30-eV levels respectively for sample B-1. Thus, if both levels were formed at the same rate, the 0.30-eV level would be populated much faster with holes than the 0.16-eV level, because its energy is lower (as far as holes are concerned) and consequently its probability of occupancy is higher. But the

*The following discussion in the test does not depend on there being a hole trap at 0.06 eV (6) above the valence band since the probability of occupancy of this level is 0.01 for B-1, 0.001 for D-8, and much lower for the 100-ohm-cm samples.

0.30-ev level is formed at a lower rate (as will be discussed in the following section) than the 0.16-ev level. In the case of the 1-ohm-cm sample, then, the Fermi level increases linearly with ϕ_f until the combination of the two factors above favors the filling of the 0.30-ev levels instead of the 0.16-ev levels. At this point, E_f begins to change with ϕ_f at a different rate and the second linear region of $\ln \sigma$ vs ϕ_f begins. Throughout the entire irradiation, of course, E_f is increasing toward the center of the gap. Finally, as saturation occurs, there is established an equilibrium which involves the density of holes left in the valence band and the density of the 0.30-ev levels being formed. Longo (14) observed more than one slope in $\ln \sigma$ vs integrated flux for 0.05-ohm-cm-initial-resistivity (presumably pulled) p-type silicon irradiated with deuterons. The end of the first linear portion of $\ln \sigma$ vs integrated dueteron flux in Longo's experiment occurred when 6×10^{17} holes/cm³ had been removed from the valence band. This would occur when approximately 10^{18} levels/cm³ which involve oxygen atoms* were filled. In the present work with zone-refined silicon (oxygen concentration less than 10^{16} /cm³), the end of the first linear portion occurs when approximately 1×10^{16} holes/cm³ are removed from the valence band. Thus, the density of holes removed by the time the second linear portion of $\ln \sigma$ vs ϕ_f begins in both pulled and zone-refined silicon seems to be very nearly the same as the available oxygen density.†

Sample D-8 - For sample D-8, the Fermi level is initially 0.27 ev (as calculated from Eq. (3) and shown in Table 1) above the valence band, and one sees from Table 1 that the probability of occupancy of the 0.16-ev and 0.30-ev levels is 0.026 and 0.72 respectively. The probability of occupancy of the 0.30-ev level is therefore 28 times higher than that of the 0.16-ev level, and the difference in production rate of the 0.16-ev and 0.30-ev levels is not sufficient to counteract the much higher probability of occupancy of the 0.30-ev levels. Thus, the single slope in the plot of $\ln p$ vs ϕ_f or of E_f vs ϕ_f for D-8 is due to a filling of the 0.30-ev levels. As saturation takes place, the change of $\ln p$ with ϕ_f is governed by the rate at which equilibrium is established between the density of defects being produced at the 0.30-ev level and the density of holes in the valence band.

Samples G-, H-, and J-100 - In the case of samples G-, H-, and J-100, the Fermi level is initially 0.34 ev or more above the valence band and the probability of occupancy of the 0.16-ev defect level is 0.0014 for G-100 and 0.0023 for H- and J-100. One can note that the probability of occupancy of the 0.30-ev level is initially 0.10 or higher and, although low, is close to a factor of 100 times that of the 0.16-ev level. Thus for these samples, as for sample D-8, the larger occupation probability of the 0.30-ev level favors its being filled in preference to the 0.16-ev level. The fact that one does not initially get a linear decrease in the curve of E_f vs ϕ_f or in $\ln p$ vs ϕ_f for these samples may be

*The lower lying 0.16-ev level could result from a hole trap due to various impurities (including boron) other than oxygen. However, since the conductivity of zone-refined silicon changes much more rapidly with irradiation than that of pulled silicon of equivalent resistivity, it seems reasonable that oxygen is the responsible agent, simply because this is the primary difference between zone-refined and pulled silicon. In addition, oxygen was chosen as the atom responsible for the trap at 0.16 ev because of the similarity between the defect levels in the upper and lower halves of the energy gap (8) and because the level 0.16 ev below the conduction band in electron-irradiated pulled n-type silicon is due to an oxygen atom and vacancy combination (11). There is some controversy as to whether neutron-irradiated n-type silicon has any discrete trapping levels. According to Rupprecht and Klein (9) there is a discrete level at 0.15 ev below the conduction band but Wertheim (5) and Sonder (15) claim there is a continuous set of levels in the upper half of the band.

†The density of holes removed during the first linear portion is also the same as the initial boron impurity concentration, and the assumed hole trapping level at 0.16 ev above the valence band could be due as much to a boron-involved level as to an oxygen-involved level. See reference 29 as to why oxygen was chosen as the impurity causing the 0.16 ev level.

due to a competition for the holes between traps formed at 0.30 ev and traps at higher energies.

If this interpretation is correct, one should find no occupied 0.16-ev levels in the 1-ohm-cm sample after the end of the first linear portion of E_f vs ϕ_f , and no occupied 0.16-ev levels at any irradiation dosage in the 8- and 100-ohm-cm samples. Two recent papers by Vavilov and Plotnikov (25) and Plotnikov et al. (26) partially confirm this "prediction." They made photoconductivity measurements at 100°K and concluded that there are levels in 100-ohm-cm zone-refined pile-irradiated (10^{13} n/cm² with an average energy of 1 Mev) p-type silicon at 0.30, 0.38, and 0.45 ev above the valence band, and no levels at 0.16 ev. To further confirm these ideas, a simple experiment could be done to locate the hole trapping levels in 1-ohm-cm zone-refined silicon after a short enough neutron irradiation such that $\ln \sigma$ is still in the first linear region.

The fact that the hole density and conductivity decreases immediately with irradiation in the case of the 100-ohm-cm samples may indicate that the deeper lying levels do not result from clusters of vacancies or interstitials. Or, if the levels are caused by clusters, the clusters are immediately formed when irradiation is begun.

Hall Coefficient Variation with Integrated Fast Flux; Hole Removal Rates

The variation of the Hall coefficient with integrated fast flux, as shown in Fig. 2, can, of course, be explained on the basis of carrier removal and by resorting to the two-carrier model as the material becomes intrinsic.

The most interesting feature of the Hall coefficient data is that R , initially positive, reaches a maximum as a function of integrated flux, and then goes negative for samples G-, H-, and J-100. Similar results were observed with pulled silicon by Longo (14) after much higher irradiation (10^{17} neutrons/cm²). With dueteron irradiation of 0.16-ohm-cm p-type (presumably pulled) silicon, Longo also observed R to go negative after 7×10^{14} deuterons/cm² (9.6 Mev) at room temperature. Klein and Straub (6), on the other hand, irradiated 60-ohm-cm (presumably pulled) p-type silicon in the Brookhaven reactor at dry ice temperature and observed the Hall coefficient and conductivity after room temperature storage extending from several days to a year. They saw no change in the sign of R with an integrated flux of 10^{14} n/cm². In the present work R becomes negative after 1.7×10^{13} and 1.4×10^{13} n/cm² for samples H- and J-100 respectively and after 7.2×10^{13} n/cm² for sample G-100.* These considerations seem to suggest that R goes through a maximum and becomes negative more rapidly for floating zone-refined silicon than for pulled silicon of equivalent resistivity.

Samples H- and J-100, irradiated at different flux rates, show similar dependence of R on integrated flux as seen in Fig. 2. Sample J-100 has a smaller maximum than H-100, probably because of a small initial increase of 10°C in temperature of the former. After a few minutes of irradiation, the temperature of J-100 was back to 72°C. However, the positions of the maxima of R occurred at the same value of ϕ_f and the positions of $R = 0$ occurred at approximately the same value of ϕ_f for both samples. Sample G-100 was irradiated at a different flux as well as at a higher temperature (100°C) than either H- or J-100. The maximum in R for G-100 occurred at an integrated flux of 4 times that for samples H- and J-100. In addition to this, R for G-100 did not become as negative as that of H- and J-100 with the integrated flux obtained during the experiment. The small difference (on an absolute scale) in irradiation temperature of 30°C between G-100

*Note from the figure legend that relative to the abscissa scale for samples H- and J-100 the scale for sample G-100 is compressed by a factor of 5.

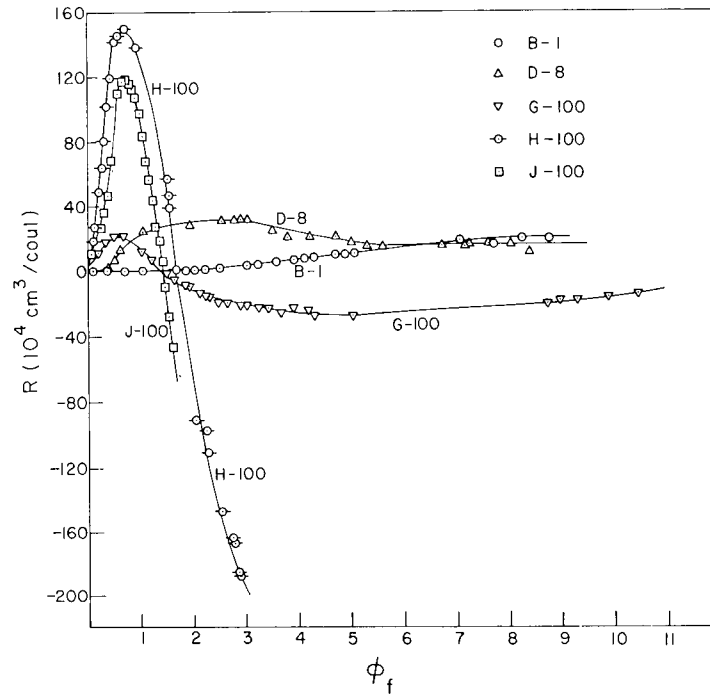


Fig. 2 - Hall coefficient R as a function of integrated fast flux ϕ_f for different p-type silicon samples irradiated at 100°C (B-1, D-8, G-100), and at 72°C (J-100, H-100). To obtain the abscissas of points in n/cm^2 , multiply the numbers along the horizontal axis by 2×10^{14} (B-1, D-8), 5×10^{13} (G-100), and 10^{13} (H-100, J-100). Some of the points at very low integrated flux have been omitted for the sake of clarity.

and H- or J-100 apparently made a large change in annealing rate and hence in the net rate of formation of the defect levels. This change was sufficient to increase the required flux necessary to bring the Hall coefficient to zero for sample G-100.

Sample D-8 exhibits a much broader peak in R vs ϕ_f and remains positive during the entire irradiation time used for this sample. In addition, the other low resistivity sample, B-1, never exhibited a maximum in R . Longo (14) observed R of 0.16-ohm-cm material to go negative after a long deuteron irradiation. This would suggest that R for the 1- and 8-ohm-cm samples eventually would have gone negative if longer irradiations had been used.

To examine the carrier removal rates we consider the Hall coefficient from which the carrier density for p-type silicon is calculated using $R = r/\rho e$, where r is the ratio of μ_H , the Hall mobility, to μ_C , the conductivity mobility. This expression can be used only during the initial period of irradiation and is not valid when the sample is approaching intrinsic behavior. According to the graph of Morin and Maita (19) for r vs T , r is about 0.71 and 0.68 for $T = 72^\circ\text{C}$ and 100°C respectively. Because of the spread in their data, a value of 0.70, independent of irradiation, has been taken to compute p , the hole density.

The carrier removal rates are listed in Table 1. The values are obtained from the first few points of a linear plot of p vs ϕ_f , which is consistent with the errors involved. These values are, of course, very approximate because of the uncertainty in the integrated fast neutron flux. The relative values, however, are significant. The initial removal rate for B-1, 80 cm^{-1} , is due primarily to holes being trapped by the 0.16-ev level. At the end of the first linear portion of $\ln \sigma$ vs ϕ_f the removal rate for sample B-1 has dropped to 40 cm^{-1} because the holes are now preferentially trapped by defects with energy levels at 0.30 ev. In the case of sample D-8 the initial removal rate of 60 cm^{-1} is lower than the initial removal rate of B-1. The fact that the holes initially are being trapped primarily by defects with energy levels at 0.16 ev for sample B-1 and at 0.30 ev for sample D-8 suggests that the 0.30-ev level defects are being formed at a lower rate than the 0.16-ev levels. The difference between the initial removal rate of D-8 and the removal rate of B-1 at the beginning of the second linear region, when, presumably, for both samples the 0.30-ev levels are being populated, may be due to the lower initial temperature of D-8. Further evidence for the lower rate of formation of the 0.30-ev levels lies in the small initial removal rate, 20 cm^{-1} , for G-100. In this sample, only the defects with energies at 0.30 ev or higher can trap holes, as discussed in the previous section. For sample G-100, the initial removal rate is lower than for D-8 and for the removal rate at the beginning of the second linear portion of B-1. This may be due to the lower probability of occupancy (0.1) of the 0.30-ev level for G-100 as well as to a competition for holes from the valence band between the 0.30-ev-level defects and higher level defects. This seems to indicate that the higher level defects are formed at an even lower rate than the 0.30-ev-level defects.

The large difference in removal rates between sample G-100 (20 cm^{-1}) irradiated at 100°C and samples H-100 (115 cm^{-1}) and J-100 (140 cm^{-1}) irradiated at 72°C indicates either a large amount of annealing or perhaps a reduction in the clustering of defects which may lower their effectiveness in trapping. Additional work has to be done to clarify this point.

Hall Mobility

The Hall mobility μ_H is shown in Fig. 3 as a function of integrated fast flux. The dashed line in Fig. 3 connects the 100°C preirradiation value of μ_H for sample D-8 with the value observed after the sample reached 100°C during the irradiation. The Hall mobility curve of H-100 was very similar to that of J-100 and has been omitted for the sake of clarity. One sees, at first, that the maximum in R as a function of ϕ_f does not result in a similar maximum in μ_H . The reason for this is that the increase in R is compensated by the decrease in σ in the early period of irradiation. μ_H appears to remain constant with ϕ_f for sample B-1, except for the scatter in the data. The Hall mobility for samples D-8 and G-, H-, and J-100 decreases with ϕ_f and, for the 100-ohm-cm samples, goes through zero and then becomes negative. One might at first think that the radiation-induced defects may increase the scattering of the holes and hence decrease μ_H . However, as indicated above, if the radiation defects exert the same influence on the conductivity as substitutional chemical impurities, the mobilities should not change much with the integrated flux received by the samples in the present work. Also, since μ_H for sample B-1 remained constant, another cause for the large decrease in μ_H must be found.

As irradiation proceeds, the hole traps cause a decrease in p . Consider the two-carrier expression for the Hall mobility:

$$\mu_H = R\sigma = \mu_h r \frac{p - n\mu_e^2/\mu_h^2}{p + n\mu_e/\mu_h} \quad (4)$$

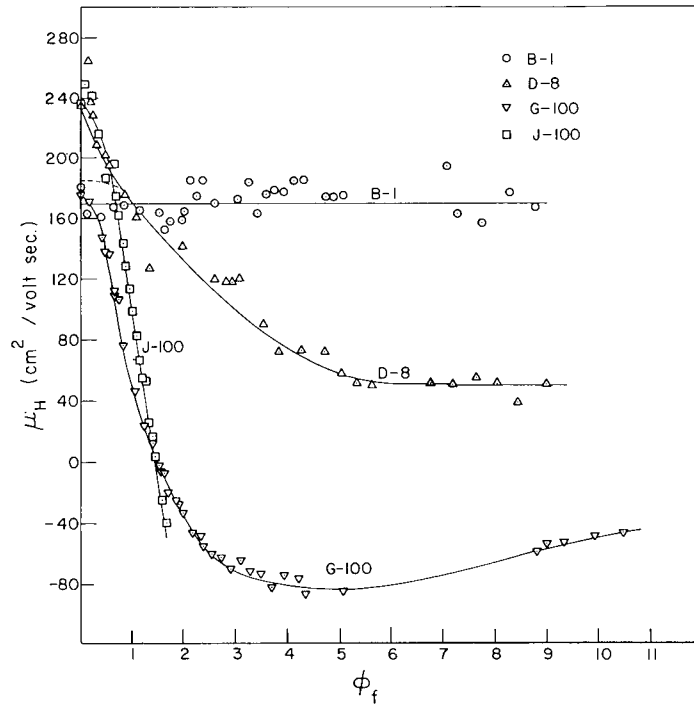


Fig. 3 - Hall mobility μ_H has a function of integrated fast flux ϕ_f for different p-type silicon samples irradiated at 100°C (B-1, D-8, G-100) and at 72°C (J-100). To obtain the abscissas of points in n/cm², multiply the numbers along the horizontal axis by 2×10^{14} (B-1, D-8), 5×10^{13} (G-100), and 10^{13} (J-100). Some of the points at very low integrated flux have been omitted for the sake of clarity.

where n is the electron density. As p decreases and approaches $n\mu_e^2/\mu_h^2$, μ_H decreases, goes through zero, and becomes negative. If the 1-ohm-cm sample had been irradiated long enough to approach intrinsic conductivity with its Hall coefficient becoming negative (both conditions were true for the 8- and 100-ohm-cm samples), then μ_H for it would have decreased with irradiation.

SUMMARY

The variations in the Hall coefficient and the conductivity of zone-refined silicon undergoing neutron irradiation are similar to those of pulled silicon except that the changes with integrated flux occur much more rapidly for the zone-refined material. The logarithm of the conductivity shows a monotonic nonlinear decrease with irradiation for the 100-ohm-cm samples, a single region of linear decrease for the 8-ohm-cm sample, and two regions of linear decrease for the 1-ohm-cm sample. For the latter sample, this effect is attributed partly to the filling of the levels which may involve oxygen atoms in some way. The initial hole removal rates are 80, 60, and 20 cm⁻¹ for the 1-, 8-, and 100-ohm-cm samples respectively at an irradiation temperature of 100°C, and 115 cm⁻¹ for one of the 100-ohm-cm samples at an irradiation temperature of 72°C. The Hall coefficient goes through a maximum and decreases for the 8- and 100-ohm-cm samples, becoming negative for the 100-ohm-cm samples. In the case of the 1-ohm-cm

sample, the Hall coefficient increases and then levels off. The Hall mobility decrease in the 8- and 100-ohm-cm samples is ascribed to a decrease in the carrier density. The Hall mobility is constant with irradiation for the 1-ohm-cm sample.

ACKNOWLEDGMENTS

The authors are deeply indebted to Dr. A. I. Schindler, who helped clarify many points by invaluable discussions and assisted in reading and correcting the manuscript. We are also grateful to Dr. E. I. Salkovitz for his guidance and support during the initial stages of this work. Several discussions with Dr. C. A. Mackliet were helpful. Finally, we want to thank the NRL reactor group headed by Dr. J. O. Elliot for their cooperation during the in-pile measurements.

REFERENCES

1. Wertheim, G. K., Phys. Rev. 105:1730 (1957)
2. Wertheim, G. K., Phys. Rev. 110:1272 (1958)
3. Hill, D. E., and Lark-Horovitz, K., Bull. Am. Phys. Soc., Ser. II, 3:142 (1958)
4. Longo, T. A., and Lark-Horovitz, K., Bull. Am. Phys. Soc., Ser. II, 2:157 (1957)
5. Wertheim, G. K., Phys. Rev. 111:1500 (1958)
6. Klein, C. A., and Straub, W. D., "Proceedings of the Third Semi-Annual Radiation Effects Symposium," Oct. 28-30, 1958, Sponsored by ARDC, USAF. Lockheed Nuclear Products, Paper 30
7. Hill, D. E., Phys. Rev. 114:1414 (1959)
8. Klein, C. A., J. App. Phys. 30:1222 (1959)
9. Rupprecht, G., and Klein, C. A., Phys. Rev. 116:342 (1959)
10. Willardson, R. K., J. App. Phys. 30:1158 (1959)
11. Watkins, G. D., and Corbett, J. W., Phys. Rev. 121:1001 (1961)
12. Corbett, J. W., Watkins, G. D., Chrenko, R. M., and McDonald, R. S., Phys. Rev. 121:1015 (1961)
13. Kaiser, W., Keck, P. H., and Lange, C. F., Phys. Rev. 101:1264 (1956)
14. Longo, T. A., Ph.D. Thesis, Purdue University, 1957 (Unpublished)
15. Sonder, E., J. App. Phys. 30:1186 (1959)
16. Buras, B., and Suwalski, J., Acta Phys. Polon. 19:115 (1960)
17. Bailey, G. C., and Williams, C. M., Rev. Sci. Instr. 32:1412 (1961)
18. See, for example, C. Kittel, "Introduction to Solid State Physics," 2nd ed., p. 351, New York: Wiley, 1956

19. Morin, F. J., and Maita, J. P., Phys. Rev. 96:28 (1954)
20. Conwell, E. M., Proc. Inst. Radio Engrs. 40:1327 (1952)
21. Billington, D. S., and Crawford, J. H., Jr., "Radiation Damage in Solids," Princeton University Press, p. 34, 1961
22. Cleland, J. W., Crawford, J. H., and Pigg, J. C., unpublished data quoted in J. H. Crawford and J. W. Cleland, "Progress in Semiconductors," vol. 2, A. F. Gibson, P. Aigrain, and R. E. Burgess, eds., London: Heywood, p. 67, 1959
23. Watkins, G. D., Corbett, J. W., and Walker, R. M., J. App. Phys. 30:1198 (1959)
24. Smith, R. A., "Semiconductors," Cambridge University Press, 1959, p. 82
25. Vavilov, V. S., and Plotnikov, A. F., Soviet Phys.—Solid State 3:1783 (1962)
26. Plotnikov, A. F., Vavilov, V. S., and Smirnov, L. S., Soviet Phys.—Solid State 3:2363 (1962)

* * *